Desalination and Water Treatment
www.deswater.com

doi:10.5004/dwt.2018.22932

132 (2018) 297–306
November

Open ended tube like hollow bio-carbon derived from banana fibre for removal of anionic and cationic dyes

Sharon Olivera[a], Krishna Venkatesh[a], Mysore Sridhar Santosh[a,b], Denis Leybo[b], Denis Kuznetsov[b], Bidarur K Jayanna[c], Inamuddin[d,e,*], Abdullah M. Asiri[d,e], Khalid Ahmed Alamry[d], Handanahally Basavarajaiah Muralidhara[a,*]

[a]*Centre for Incubation, Innovation, Research and Consultancy (CIIRC), Jyothy Institute of Technology, Thataguni, off Kanakapura Road, Bangalore 560 082, Karnataka, India, email: olivera333sharon@gmail.com (S. Olivera), igit@rediffmail.com (K. Venkatesh), santoshgulwadi@gmail.com (M.S. Santosh), hb.murali@gmail.com (H.B. Muralidhara)*
[b]*Department of Functional Nanosystems and High-Temperature Materials, National University of Science and Technology "MISiS", Leninskiy Pr. 4, Moscow, 119049, Russia, email: leybodv@gmail.com (D. Leybo), dk@misis.ru (D. Kuznetsov)*
[c]*Department of Chemistry, B.N.M. Institute of Technology, Bangalore 560 070, Karnataka, India, email: ninge1973@gmail.com (B.K Jayanna)*
[d]*Chemistry Department, Faculty of Science, King Abdulaziz University, Jeddah 21589, Saudi Arabia, email: inamuddin@rediffmail.com (Inamuddin), khalid_alamry@yahoo.com (K.A. Alamry)*
[e]*Centre of Excellence for Advanced Materials Research, King Abdulaziz University, Jeddah 21589, Saudi Arabia, email: aasiri2@kau.edu.sa (A.M. Asiri)*

Received 20 March 2018; Accepted 6 August 2018

ABSTRACT

The hollow tube-like banana fibre carbon (BFC) materials was utilized for adsorptive removal of toxic cationic dyes such as methyl violet (MV) and crystal violet (CV), and anionic dyes such as methyl orange (MO) and alizarin red S (ARS) from water. Scanning electronic microscopy (SEM) images revealed the hollow ends of the carbons were prominent. The chemical composition of BFC indicated that the carboxylate groups majorly contributed to the adsorption capacity. Langmuir isotherm and pseudo-first-order kinetics were effectively fitted to adsorption results. The maximum adsorption capacities were equal to 85.65, 78.95, 65.78 and 65.07 mg/g for MV, MO, CV and ARS, respectively. The biocarbon of banana fibre could be a good choice for water treatment due to its attractive adsorption performance.

Keywords: Banana fibre; Carbon; Porous; Cationic dye; Anionic dye

1. Introduction

Water pollution by synthetic dyes is a cause of apprehension as they can potentially contaminate surface water and groundwater. In order to meet the increasing demands of growing population, dye consuming industries such as food, textile, leather, paper, cosmetics, pulp mills, plastic, printing and carpet are expanding exponentially [1–3]. It is estimated that over 10,000 types of textile dyes alone are produced worldwide to an amount of 7.1×10^5 metric tons per year. Approximately 10–25% of the dyes thus produced are lost during the process of dyeing and 2–20% of them are discharged directly into the water stream [4]. These dye effluents cause harmful effects on aquatic communities by impeding the light penetration, retarding photosynthesis and inhibiting re-oxygenation capacity responsible for aquatic plant growth. They also affect human health by causing allergic dermatitis, cancerous and mutagenic effects [5,6]. Several measures are undertaken to arrest the dye contamination at its source. However, alternate approaches

*Corresponding author.

for removal of dyes have been researched as it is not easy to avoid their discharge into water in the current scenario. Among them, adsorption is a promising technology because of its simplicity of operation, low-cost and efficient removal of contaminant even at low concentrations [7].

A large number of materials have been utilized for the adsorption of dyes from aqueous solutions. Metallic, bio-based, organic and inorganic adsorbents have been investigated for their potential role in eliminating dyes; biomass-based carbons [8,9], nanometal oxides [10,11], clays [12,13], cellulose and chitosan composites [7,14] etc., being prominent. However, adsorbents generally face challenges in terms of cost, efficiency and selectivity towards the target contaminant. Hence, there is a great scope for the exploration of novel adsorbents for treatment of wastewater.

Abundance and cost-effective nature of biomass such as crop residues and agricultural byproducts offer great scope for the adsorption of dyes. A good number of materials such as sugarcane bagasse, coconut shell powder, rice husk, coir pith and sawdust have been employed in the raw form [15,16]. Chemical and physical modifications were also carried out in certain instances to improve the adsorption capacity. For example, ethylenediamine modified rice hull showed adsorption capacities of 14.68 and 60.24 mg/g for basic blue 3 and reactive orange 16 respectively which corresponded to 4.5 and 2.4 fold increase [17].

Generally, the adsorbent biomasses consist of cellulose, lignin and hemicellulose constituents. Although biomasses have been found to be efficient for sorption of dyes, they face problems due to protective cover which hinders permeation of chemicals, presence of recalcitrant lignin, and huge variations in structure and properties [18]. Hence, the carbonization of biomass resulting in porous structures desirable for high adsorption of contaminants is a preferred method [19].

Banana fibres are natural fibres that are abundantly present. They are derived from perennial herb of banana plant. They are ligno-cellulosic fibres which are recyclable and biodegradable. It would be advantageous to use them for water treatment applications. Hence, in this work, banana fibres were carbonized and utilized to remove four dyes namely MV, MO, CV and ARS from water both by adsorption. The application of carbons obtained from banana fibres without any further activation could be added advantage as it can be energy efficient and cost-effective. The structure and properties of banana fibre carbon (BFC) were characterized and studied for adsorption of dyes at different concentrations. The potential of BFC towards water treatment was determined by comparing it with some of the biomass based carbons reported in literature.

2. Materials and methods

2.1. Materials

Banana fibres were obtained from Tamilnadu Agricultural University, Coimbatore, India. The dyes of MV, MO, CV and ARS were procured from Bangalore Scientific, Bengaluru, India. Sodium hydroxide pellets (NaOH) and hydrochloric acid (HCl) were purchased from Manasa Agencies, Bengaluru, India. All chemicals were used without further purification. Double distilled water was utilized for all the experiments.

2.2. Methods

The BFC samples were fabricated by carbonization of raw banana fibres. A fixed quantity of banana fibres was calcined in N_2 atmosphere at 550°C for 1 h. They were cooled to room temperature and stored for adsorption studies. MV, MO, CV and ARS dyes were prepared in concentrations of 25, 50, 75 and 100 mg/L for the adsorption experiments. Adsorption tests were done by mixing a fixed amount of BFC with the dye solutions. The mixture was stirred for 180 min at speed of 300 rpm. The sample was separated by filtration and colored filtrates were subjected to colorimetric analysis using a UV-Visible spectrophotometer at the wavelengths of 585, 525, 588 and 423 nm for MV, MO, CV and ARS, respectively. The decrease in intensity of color indicated the removal of dyes from the solution. The screening for the determination of optimum pH was conducted using dilute HCl and NaOH for adjusting pH.

2.3. Characterizations

The morphologies of BFC were characterized by scanning electron microscopy (SEM, HITACHI, SU3500). Image J software was used to determine diameter of the porous structures. The surface functionalities of BFC were evaluated by Fourier transform infra-red (FT-IR) technique on a Shimadzu ATR spectrophotometer. The spectrum was recorded from 4000 to 400 cm^{-1}. A total of 64 scans were done with a resolution of 4 cm^{-1}. The physico-chemical characterization was performed on a NOVA 1200 (Quantachrome, USA) instrument. BFC was degassed in vacuum at 200°C overnight prior to the analysis. The Brunauer–Emmett–Teller (BET) surface area, total pore volume and the average pore size of the samples were determined by N_2 adsorption studies at 77.4 K. The thermal decomposition in the temperature range from room temperature to 800°C of BFC was studied using thermosgravimetric analyzer instruments, USA (SDT Q600) with Ar flow rate of 100 mL/min and heat ramping of 10°C/min. Raman studies were conducted on Thermo science dxr spectrometer using 5 MW, 532 nm laser with exposition of 3 s in the range of 650–2250 cm^{-1}.

3. Results and discussion

3.1. Characterization of BFC

The microstructure of the material can play a vital role in the removal of cationic and anionic dyes under investigation. As shown in Fig. 1A and Fig. 1B, micrometer-sized tube like structure was observed for BFC in accordance with the literature [20]. The diameters of the porous structures varied from 1.88 to 12.08 μm as shown in Fig. 1A. The morphology of BFC was further revealed by SEM images as shown in Figs. S1A–S1C (Supplementary Information). The open ended tube-like morphology of BFC can facilitate the easy access to the cationic and anionic dyes used in the study to be accommodated to large extent.

Fig. S2 (Supplementary Information) shows the plots of N_2 adsorption-desorption isotherms and pore diameter versus pore volume. Type I isotherm (International Union of Pure and Applied Chemistry classification) with an open loop was observed which is a characteristic of very narrow

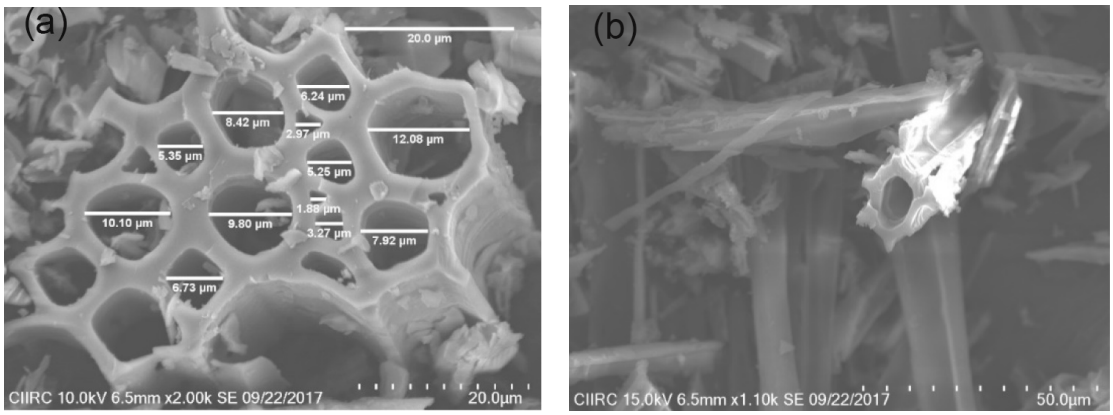

Fig. 1. SEM images of (A) BFC 20 µm, (B) BFC at 50 µm.

slit pores or bottle shaped pores. It was observed that BFC was consisted of micropores and mesopores. The specific surface area value of BFC was equal to 8.09 m^2/g. Although the surface area of BFC is small, the presence of large number of functional groups may aid in the larger uptake of cationic and anionic dyes based on their feasible interactions at optimum pH values.

In the Raman spectra given in Fig. S3 (Supplementary Information), the presence of D and G bands were observed at 1354 and 1585 cm^{-1}, respectively. In general, D band represents disordered carbon that corresponds to turbostatic carbon sheets or minor graphitic domains while G band is ascribed to in-plane displacement of carbons within hexagonal carbon layers. The I_D/I_G ratio was determined to be equal to 0.85. This value which is lower than 1 is an indication of higher extent of graphitization compared to the number of defects present in BFC [21]. This can be helpful in promoting adsorption of the contaminants by enhancing π-π electron donor-acceptor interactions among BFC and the dyes under investigation [22].

Thermal degradation profile of raw banana fibres is presented in Fig. S4 (Supplementary Information). About 9% of weight loss observed up to 100°C was attributed to loss of physically adsorbed water. The major weight loss of about 57% between 180–650°C was associated with the decomposition of hemicellulose. Degradation of lignin was not seen because of the complex structure and its typical gradual weight loss profile between 100–800°C [23]. Differential scanning calorimetry (DSC) of banana fibre showed major peak at 320°C which could be ascribed to degradation of α-cellulose [24].

3.2. Adsorption experiments

3.2.1. Influence of initial concentration of dyes on removal efficiency

The effect of initial concentration of adsorbate on the removal efficiency of MV, MO, CV and ARS was examined as shown in Fig. 2. It is a common observation for all the dyes that removal capacity was high when the initial concentration was 25 mg/L. It declined as the concentration was increased to 50, 75 and 100 mg/L. This behavior was attributed to the availability of large number of active adsorption sites on the adsorbent at lower initial concentration of the adsorbate. The same number of active sites would be available for the higher concentrations of the adsorbate, thus causing the drop in removal efficiency. It was also seen that the removal of dyes was swift in the first 40 min accounting for more than 60% of the removal capacity which became steadier as the contact time was increased to 180 min. This is again due to the rapid filling up of active sites in the initial stage of adsorption.

3.2.2. pH effect

pH of the dye solution plays a significant role in deciding the adsorption performance. The influence of pH on the removal percentage of the dyes was investigated and results are presented in Fig. 3. In the case of MV, the percentage removal increased with the pH of the dye solution and maximum removal efficiency was observed at pH of 9 becoming stable on further increase of pH values. The difference in removal percentage at different pH values could be attributed to the extent of ionization/dissociation of MV and surface charge of BFC adsorbent. At lower pH values, electrostatic repulsion between cationic MV and positively charged BFC predominates while at higher pH values, electrostatic attraction prevails as surface of BFC would carry negative charge. This result is in agreement with the reports published in literature [25,26]. It was observed that pH of MO solution had negligible impact on the removal efficiency of BFC. The reasons for this are that MO can exist in two different chemical forms, that is, anthraquinone or azo bond based on the pH values. The dominance of either of the forms at different pH contributes to the sort of behavior observed for MO dye removal [27,28]. The variation of CV with pH showed a pattern which was similar to the case of MV. The electrostatic repulsion at acidic pH and electrostatic attraction at basic pH were the reasons for the lower and higher removal percentages, respectively [29]. ARS showed high percentage removal at acidic pH which then decreased as the pH of the solution changed to basic. This can be explained by interaction of anionic charge of ARS with the positively charged surface of BFC at acidic pH and electrostatic repulsion at basic values as the BFC surface would carry negative charge [30].

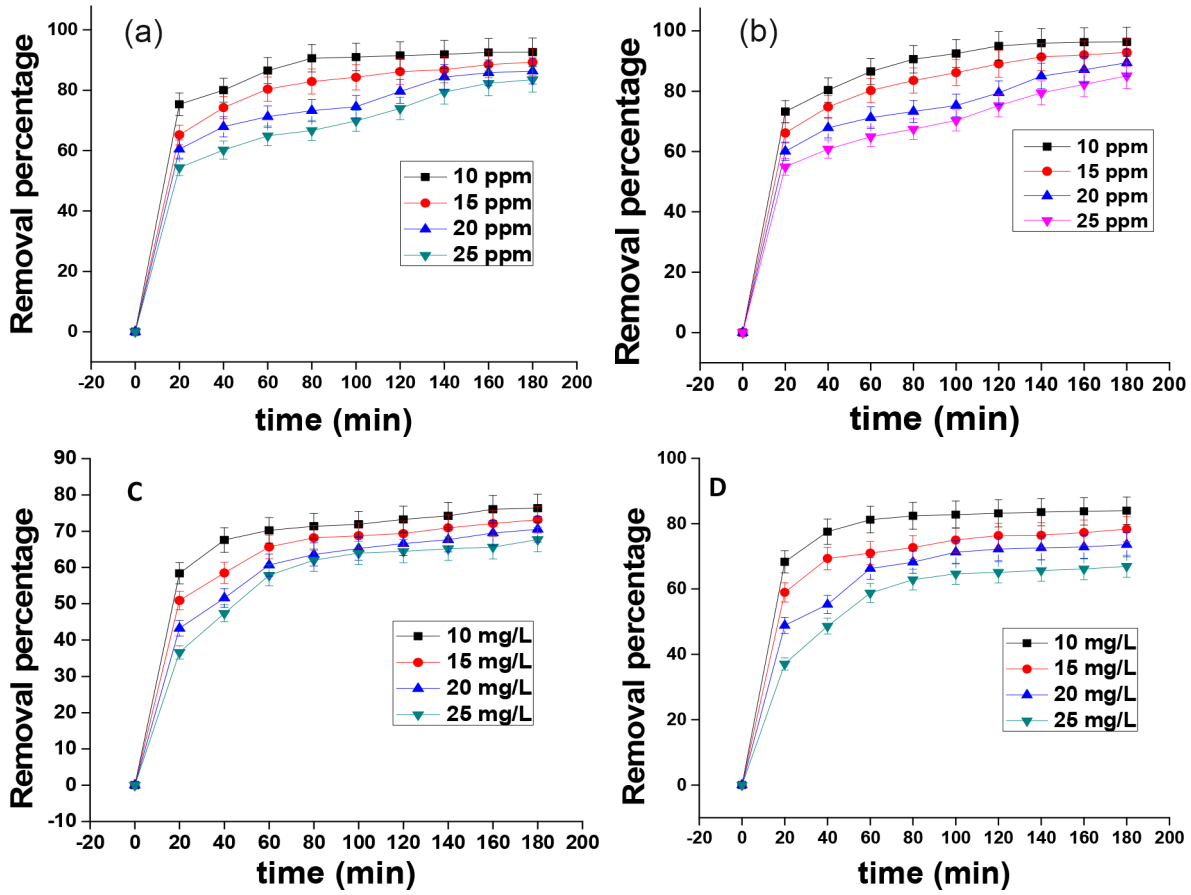

Fig. 2. Influence of initial concentration of (A) MV (B) MO (C) CV and (D) ARS removal efficiency.

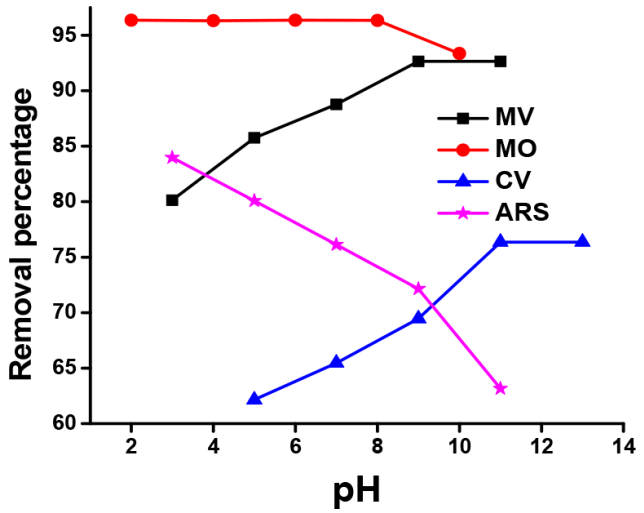

Fig. 3. Variation of removal efficiency of BFC with pH of different dyes utilized in the study.

3.2.3. Isotherms

Adsorption isotherms are practical in identifying the distribution profile of the adsorbate between liquid and solid phases when adsorption process attains equilibrium [31,32]. The calculation of adsorption isotherms was done by Langmuir and Freundlich models. The Langmuir equation assumes mono-layer adsorption of the adsorbate on the homogeneous surface of the adsorbent and states that there is no interaction between the neighboring adsorbent molecules whereas Freundlich model predicts multi-layer coverage of the adsorbate on the heterogeneous adsorbent surface. Langmuir isotherm can be expressed by the following equations:

$$Qe = \frac{K_L C_e}{1 + a_L C_e} \quad (1)$$

where 'Q_e' and 'C_e' represent equilibrium adsorption capacity and equilibrium adsorbate concentration, respectively. 'K_L' and 'a_L' denote Langmuir constants. Theoretical maximum adsorption capacity, 'Q_{max}', can be found from K_L/a_L.

The linear form of Freundlich equation is represented as:

$$\log Q_e = \frac{1}{n_F} \log C_e + \log K_F \quad (2)$$

where 'C_e' and 'Q_e' are equilibrium adsorbent concentration and equilibrium adsorption capacity, respectively. 'K_F' and 'n_F' are Freundlich constants.

The results displayed in Table 1 show that the adsorption data were in better agreement with Langmuir model with R^2 values higher than 0.998 compared to Freundlich model with

Table 1
Langmuir and Freundlich parameters for MV, MO, CV and ARS dyes removal

	Langmuir constants			Freundlich constants		
Contaminant	Q_0 (mg/g)	K_L (L/mg)	R^2	K_F (mg/g)	n_F	R^2
Methyl violet	85.65	0.18	0.99853	71.05	2.68	0.94658
Methyl orange	78.95	0.15	0.99679	65.25	2.76	0.95623
Crystal violet	65.78	0.12	0.99122	51.26	2.64	0.95642
Alizarin red S	65.07	0.10	0.99495	40.82	2.85	0.96256

Table 2
Comparison of adsorption capacities of BFC with few bio-based adsorbent materials reported in literature

Sl No	Adsorbent	Dye	Adsorption capacity (mg/g)	Reference
1	Sunflower seed hull	Methyl violet	92.59	[33]
2	Silver nanoparticles modified carbon	Methyl orange	27.48	[34]
3	Tomato waste nanoporous carbon	Crystal violet	68.97	[35]
4	Palm kernel fibre	Crystal violet	78.9	[36]
5	Banana fibre powder	Direct red 23	21.05	[37]
6	Banana fibre powder	Direct red 80	36.50	[37]
7	Multiwalled carbon nanotubes	Malachite green	198.41	[38]
8	Multiwalled carbon nanotubes	Methyl orange	178.21	[38]
8	Banana fibre carbon	Methyl violet	85.65	This work
9	Banana fibre carbon	Methyl orange	78.95	This work
10	Banana fibre carbon	Crystal violet	65.78	This work
1	Banana fibre carbon	Alizarin red S	65.07	This work

R^2 values lower than 0.94. The Langmuir adsorption capacities for MV, MO, CV and ARS were equal to 85.65, 78.95, 65.78 and 65.07 mg/g, respectively. These adsorption capacities were significant because these were determined for BFC fabricated without any activation process. Chemical or physical activations on BFC may be carried out to obtain higher adsorption capacities. A comparison of adsorption capacities of BFC with some of the carbon based adsorbents for removal of dyes reported in the literature is presented in Table 2.

3.2.4. Adsorption kinetics

The kinetics of removal of dye provides useful insights about adsorption rate which governs the residence time of dye on the solid-liquid interface. Kinetic factors also come into play while designing and modeling adsorption systems. In the current study, kinetic investigations were carried out by measuring the absorbance of filtrate obtained upon adsorption in intervals of 20 min as shown in Table 3. Models such as Lagergren pseudo-first-order kinetic model, pseudo-second-order model and intra-particle diffusion model were applied for the kinetic data results [39,40]. They are represented by the following equations:

$$\log\left(Q_e - Q_t\right) = \log Q_e - \frac{k_1}{2.303}t \tag{3}$$

$$\frac{t}{Q_t} = \frac{1}{k_2 Q_e^2} + \frac{1}{Q_e}t \tag{4}$$

$$Q_t = k_3 t^{1/2} \tag{5}$$

The kinetic data corroborated well with Lagergren pseudo-first-order model with regression coefficient (R^2) having values above 0.998 whereas lower R^2 values in the case of pseudo-second-order model implied poor adherence. There was a close agreement of Q_{ecal} and Q_{eexp} for Lagergren pseudo-first-order model. This indicates the adsorption mechanism primarily involved physisorption than the chemical sorption.

The intra-particle diffusion model assumes that if a graph of the amount of contaminant adsorbed (Q_t) versus square root of time ($t_{1/2}$) is linear, and if these lines pass through the origin, then adsorption depends only on intra-particle diffusion. However, Fig. S5 showed that the plots were not linear over entire time range and instead, can be separated into multi-linear curves, implying that multiple steps were involved in adsorption process. It can be concluded that adsorption of MV, MO, CV and ARS on BFC involved more than one process, and intra-particle diffusion was not the rate-limiting step. This behavior is in agreement with studies reported in the literature [41–43].

3.2.5. Dye removal mechanism

Even though physisorption was the major contributor to adsorption, chemical sorption also played significant role as confirmed by the FT-IR spectrum

Table 3
Lagergren and pseudo-second-order kinetic parameters for MV, MO, CV and ARS

Models	Parameters	Methyl violet dye concentration (mg/L)				Methyl orange dye concentration (mg/L)			
		10	15	20	25	10	15	20	25
Lagergren kinetic model	Q_{ecal} (mg/g)	30.87	44.63	57.55	72.33	32.13	46.41	58.79	72.33
	k_1 (min^{-1})	0.078	0.075	0.080	0.075	0.092	0.094	0.87	0.075
	R^2	0.99952	0.99899	0.99989	0.99998	0.99912	0.99921	0.99931	0.99998
	Q_{eexp} (mg/g)	30.88	44.64	57.59	72.35	32.12	46.41	59.61	72.35
Pseudo-second order kinetic model	Q_{ecal} (mg/g)	32.13	46.41	58.79	72.33	30.87	44.63	57.55	72.33
	k_2 (min^{-1})	0.071	0.063	0.081	0.088	0.075	0.075	0.084	0.088
	R^2	0.95126	0.96214	0.92545	0.90365	0.91235	0.92467	0.90243	0.90365
	Q_{eexp} (mg/g)	32.12	46.41	59.61	72.35	30.88	44.45	57.39	72.05

Q_e and Q_t are the amounts of adsorbate adsorbed (mg g^{-1}) at equilibrium and at contact time t (min) respectively, and k_1 is the pseudo-first-order rate constant (min^{-1}). k_2 is the pseudo-second-order rate constant (min^{-1}).

Models	Parameters	Crystal violet dye concentration (mg/L)				Alizarin red S dye concentration (mg/L)			
		10	15	20	25	10	15	20	25
Lagergren kinetic model	Q_{ecal} (mg/g)	25.41	36.62	46.95	61.69	24.23	39.11	48.85	60.96
	k_1 (min^{-1})	0.069	0.084	0.082	0.089	0.087	0.086	0.88	0.99
	R^2	0.99889	0.99867	0.99859	0.99979	0.99987	0.99950	0.99977	0.99968
	Q_{eexp} (mg/g)	25.45	36.60	47.03	61.80	24.23	39.17	49.03	61.30
Pseudo-second order kinetic model	Q_{ecal} (mg/g)	24.20	32.14	38.25	42.87	21.77	30.25	38.17	49.24
	k_2 (min^{-1})	0.049	0.051	0.067	0.042	0.075	0.062	0.072	0.071
	R^2	0.91478	0.93415	0.90444	0.90781	0.82478	0.92477	0.83699	0.91742
	Q_{eexp} (mg/g)	25.45	36.60	47.03	61.80	24.23	39.17	49.03	61.30

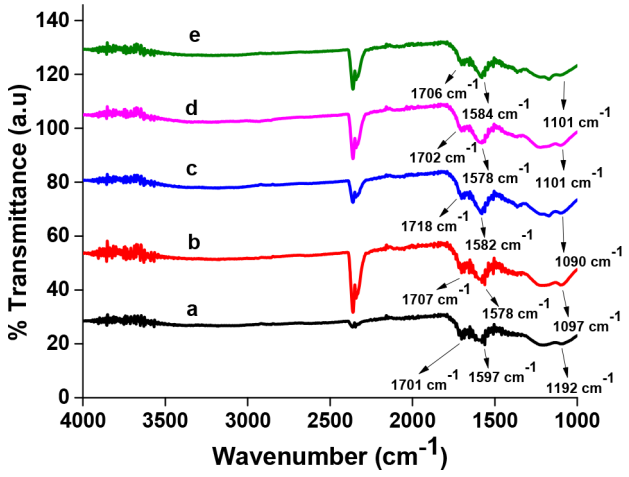

Fig. 4. FT-IR spectrum of (a) BFC (b) ARS (c) CV (d) MO (e) MV.

of dye adsorbed BFC as shown in Fig. 4. BFC originally had broad peak at 3314 cm^{-1} corresponding to absorbed hydroxyl group. The absorptions at 1701, 1597 and 1192 cm^{-1} could be attributed to C=O, C=C and C-O, respectively. The functional groups were expected to interact electro statically with the dyes leading to their removal from contaminated water. Upon adsorption of dyes on BFC, the shift of C=O and C-O groups by few wavenumber units confirmed minor chemisorption taking plus which additionally contributed to adsorption capacity of BFC.

3.2.6. Reusability of BFC

The regeneration properties of BFC material were investigated by treating the dye adsorbed BFC with 0.01 N HCl. It was found that the removal efficiency decreased from 89.29, 76.36, 92.81 and 78.33% to 81.28, 69.75, 85.25 and 70.48%, respectively, for MV, CV, MO and ARS respectively after three cycles of adsorption-desorption. Further desorption for BFC may be obtained by using higher concentration of acid, higher temperature etc. However, a lower pH desorbing media usually tends to degrade the adsorbent matrix which interferes with the analysis [18].

4. Conclusions

Bio-based carbons of banana fibres with hollow ends were fabricated in the present study and investigated for their ability to remove two cationic and two anionic dyes. The adsorbent exhibited favorable adsorption capacity towards all the dyes and recorded adsorption capacities of 85.65, 78.95, 65.78 and 65.07 mg/g for methyl violet, methyl orange, crystal violet and alizarin red S, respectively. This biocarbon of banana fibre is a potential adsorbent for dye removal as it showed good adsorption performance without any type of activation.

Acknowledgements

Authors thank the Centre for Incubation, Innovation, Research and Consultancy, Jyothy Institute of Technology and Sri Sringeri Sharadha Peetam for supporting this research.

Supplementary material

Fig. S1–S5

Notes

The authors declare that there is no competing financial interest.

References

[1] M.D.G. de Luna, E.D. Flores, D.A.D. Genuino, C.M. Futalan, M.W. Wan, Adsorption of Eriochrome Black T (EBT) dye using activated carbon prepared from waste rice hulls—optimization, isotherm and kinetic studies, J. Taiwan Inst. Chem. Eng., 44 (2013) 646–653.
[2] A. Regti, M.R. Laamari, S.-E. Stiriba, M. El Haddad, The potential use of activated carbon prepared from Ziziphus species for removing dyes from waste waters, Appl. Water Sci., 7 (2017) 4099–4108.
[3] F. Marrakchi, M.J. Ahmed, W. Khanday, M. Asif, B. Hameed, Mesoporous carbonaceous material from fish scales as low-cost adsorbent for reactive orange 16 adsorption, J. Taiwan Inst. Chem. Eng., 71 (2017) 47–54.
[4] A. Baban, A. Yediler, N.K. Ciliz, Integrated water management and CP implementation for wool and textile blend processes, CLEAN–Soil, Air, Water., 38 (2010) 84–90.
[5] A.N. Ejhieh, M. Khorsandi, Photodecolorization of Eriochrome Black T using NiS–P zeolite as a heterogeneous catalyst, J. Hazard. Mater., 176 (2010) 629–637.
[6] A. Khalid, M. Zubair, A comparative study on the adsorption of Eriochrome Black T dye from aqueous solution on graphene and acid-modified graphene, Arab. J. Sci. Eng., (2017) 1–13.
[7] S. Olivera, H.B. Muralidhara, K. Venkatesh, V.K. Guna, K. Gopalakrishna, Y. Kumar, Potential applications of cellulose and chitosan nanoparticles/composites in wastewater treatment: A review, Carbohydr. Polym., 153 (2016) 600–618.
[8] T. Maneerung, J. Liew, Y. Dai, S. Kawi, C. Chong, C.-H. Wang, Activated carbon derived from carbon residue from biomass gasification and its application for dye adsorption: kinetics, isotherms and thermodynamic studies, Bioresour. Technol., 200 (2016) 350–359.
[9] S. Sangon, A.J. Hunt, T.M. Attard, P. Mengchang, Y. Ngernyen, N. Supanchaiyamat, Valorisation of waste rice straw for the production of highly effective carbon based adsorbents for dyes removal, J. Clean Prod., 172 (2018) 1128–1139.
[10] P. Xu, G.M. Zeng, D.L. Huang, C.L. Feng, S. Hu, M.H. Zhao, C. Lai, Z. Wei, C. Huang, G.X. Xie, Use of iron oxide nanomaterials in wastewater treatment: a review, Sci. Total Environ., 424 (2012) 1–10.
[11] L. Ge, W. Wang, Z. Peng, F. Tan, X. Wang, J. Chen, X. Qiao, Facile fabrication of Fe@MgO magnetic nanocomposites for efficient removal of heavy metalf ion and dye from water, Powder Technol., 326 (2018) 393–401.
[12] G.W. Beall, The use of organo-clays in water treatment, Appl. Clay Sci., 24 (2003) 11–20.
[13] A. Kausar, M. Iqbal, A. Javed, K. Aftab, H.N. Bhatti, S. Nouren, Dyes adsorption using clay and modified clay: A review, J. Mol Liq., 256 (2018) 395–407.
[14] X. Zheng, X. Li, J. Li, L. Wang, W. Jin, Y. Pei, K. Tang, Efficient removal of anionic dye (Congo red) by dialdehyde microfibrillated cellulose/chitosan composite film with significantly improved stability in dye solution, Int. J. Biol. Macromol., 107 (2018) 283–289.
[15] G. Crini, Non-conventional low-cost adsorbents for dye removal: a review, Bioresour. Technol., 97 (2006) 1061–1085.
[16] M. Paredes-Laverde, J. Silva-Agredo, R.A. Torres-Palma, Removal of norfloxacin in deionized, municipal water and urine using rice (*Oryza sativa*) and coffee (*Coffea arabica*) husk wastes as natural adsorbents, J. Environ. Manage., 213 (2018) 98–108.
[17] S. Ong, C. Lee, Z. Zainal, Removal of basic and reactive dyes using ethylenediamine modified rice hull, Bioresour. Technol., 98 (2007) 2792–2799.
[18] M. Ilangovan, V. Guna, S. Olivera, A. Ravi, H.B. Muralidhara, M. Santosh, N. Reddy, Highly porous carbon from a natural cellulose fiber as high efficiency sorbent for lead in waste water, Bioresour. Technol., 245 (2017) 296–299.
[19] R. Gong, J. Ye, W. Dai, X. Yan, J. Hu, X. Hu, S. Li, H. Huang, Adsorptive removal of methyl orange and methylene blue from aqueous solution with finger-citron-residue-based activated carbon, Ind. Eng. Chem. Res., 52 (2013) 14297–14303.
[20] V. Subramanian, C. Luo, A. Stephan, K. Nahm, S. Thomas, B. Wei, Supercapacitors from activated carbon derived from banana fibers, J. Phys. Chem. C., 111 (2007) 7527–7531.
[21] J.G. Li, C.Y. Tsai, S.-W. Kuo, Fabrication and characterization of inorganic silver and palladium nanostructures within hexagonal cylindrical channels of mesoporous carbon, Polymers., 6 (2014) 1794–1809.
[22] Y. Liu, X. Liu, W. Dong, L. Zhang, Q. Kong, W. Wang, Efficient Adsorption of Sulfamethazine onto modified activated carbon: a plausible adsorption mechanism, Sci. Rep., 7 (2017) 12437.
[23] A.P.B. Gonçalves, C.S.d. Miranda, D.H. Guimarães, J.C.d. Oliveira, A.M.F. Cruz, F.L.B.M.d. Silva, S. Luporini, N.M. José, Physicochemical, mechanical and morphologic characterization of purple banana fibers, Mater. Res., 18 (2015) 205–209.
[24] E. Abraham, B. Deepa, L. Pothan, M. Jacob, S. Thomas, U. Cvelbar, R. Anandjiwala, Extraction of nanocellulose fibrils from lignocellulosic fibres: A novel approach, Carbohydr. Polym., 86 (2011) 1468–1475.
[25] P. Phatai, S. Utara, N. Hatthapanit, Removal of methyl violet by adsorption onto activated carbon derived from coffee residues, in: Advanced Materials Research, Trans Tech Publ., 2014, pp. 710–714.
[26] P. Phatai, R. Srisomang, Characteristics and performance of a mesoporous cerium-aluminum-silver mixed oxide for removal of methyl violet dye, Sains Malaysiana., 45 (2016) 1477–1485.
[27] J. Ma, F. Yu, L. Zhou, L. Jin, M. Yang, J. Luan, Y. Tang, H. Fan, Z. Yuan, J. Chen, Enhanced adsorptive removal of methyl orange and methylene blue from aqueous solution by alkali-activated multiwalled carbon nanotubes, ACS. Appl. Mater. Interfaces., 4 (2012) 5749–5760.
[28] B. Doshi, A. Ayati, B. Tanhaei, E. Repo, M. Sillanpää, Partially carboxymethylated and partially cross-linked surface of chitosan versus the adsorptive removal of dyes and divalent metal ions, Carbohydr. Polym., (2018).
[29] K. Mohanty, J.T. Naidu, B. Meikap, M. Biswas, Removal of crystal violet from wastewater by activated carbons prepared from rice husk, Ind. Eng. Chem. Res., 45 (2006) 5165–5171.
[30] F. Fu, Z. Gao, L. Gao, D. Li, Effective adsorption of anionic dye, alizarin red S, from aqueous solutions on activated clay modified by iron oxide, Ind. Eng. Chem. Res., 50 (2011) 9712–9717.
[31] Y. Zhuang, F. Yu, J. Ma, J. Chen, Facile synthesis of three-dimensional graphene–soy protein aerogel composites for tetracycline adsorption, Desal. Water Treat., 57 (2016) 9510–9519.
[32] R. Foroutan, H. Esmaeili, M. Abbasi, M. Rezakazemi, M. Mesbah, Adsorption behavior of Cu (II) and Co (II) using chemically modified marine algae, Environ. Technol., (2017) 1–9.
[33] N.M. Mahmoodi, M. Arami, N.Y. Limaee, N.S. Tabrizi, Kinetics of heterogeneous photocatalytic degradation of reactive dyes in an immobilized TiO_2 photocatalytic reactor, J. Colloid. Interface. Sci., 295 (2006) 159–164.

[34] Q.-X. Zeng, G.-C. Xu, L. Zhang, H. Lin, Y. Lv, D.-Z. Jia, Porous CuO nanofibers derived from a Cu-based coordination polymer as a photocatalyst for the degradation of rhodamine B, New J. Chem., 42 (2018) 7016–7024.
[35] N. Gholami, B. Ghasemi, B. Anvaripou, S. Jorfi, Enhanced photocatalytic degradation of furfural and a real wastewater using UVC/TiO_2 nanoparticles immobilized on white concrete in a fixed-bed reactor, J. Ind. Eng. Chem., 62 (2018) 291–301.
[36] T. Liu, L. Wang, X. Lu, J. Fan, X. Cai, B. Gao, R. Miao, J. Wang, Y. Lv, Comparative study of the photocatalytic performance for the degradation of different dyes by $ZnIn_2S_4$: adsorption, active species, and pathways, RSC Adv., 7 (2017) 12292–12300.
[37] M. Ge, Photodegradation of rhodamine B and methyl orange by Ag_3PO_4 catalyst under visible light irradiation, Chinese J. Catalysis., 35 (2014) 1410–1417.
[38] D.P. Dutta, R. Venugopalan, S. Chopade, Manipulating carbon nanotubes for efficient removal of both cationic and anionic dyes from wastewater, Chemistry Select., 2 (2017) 3878–3888.
[39] B. Wanassi, I.B. Hariz, C.M. Ghimbeu, C. Vaulot, M.B. Hassen, M. Jeguirim, Carbonaceous adsorbents derived from textile cotton waste for the removal of Alizarin S dye from aqueous effluent: kinetic and equilibrium studies, Environ. Sci. Pollut. Res., 24 (2017) 10041–10055.
[40] A. Kupeta, E. Naidoo, A. Ofomaja, Kinetics and equilibrium study of 2-nitrophenol adsorption onto polyurethane cross-linked pine cone biomass, J. Clean Prod., (2018).
[41] K.G. Bhattacharyya, A. Sharma, Adsorption of Pb (II) from aqueous solution by *Azadirachta indica* (Neem) leaf powder, J. Hazard. Mater., 113 (2004) 97–109.
[42] K. Mahmoudi, N. Hamdi, A. Kriaa, E. Srasra, Adsorption of methyl orange using activated carbon prepared from lignin by $ZnCl_2$ treatment, Russ. J. Phys. Chem A., 86 (2012) 1294–1300.
[43] E.N. El Qada, S.J. Allen, G.M. Walker, Adsorption of methylene blue onto activated carbon produced from steam activated bituminous coal: a study of equilibrium adsorption isotherm, Chem. Eng. J., 124 (2006) 103–110.

Supplementary

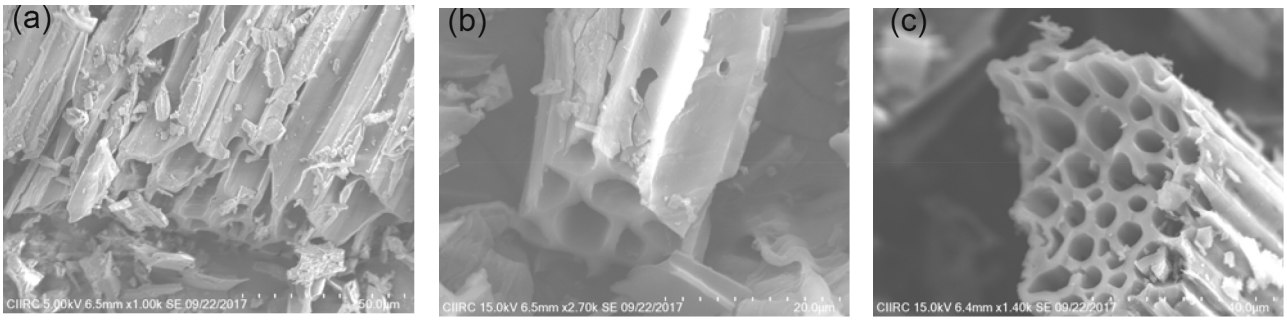

Fig. S1. SEM images of BFC.

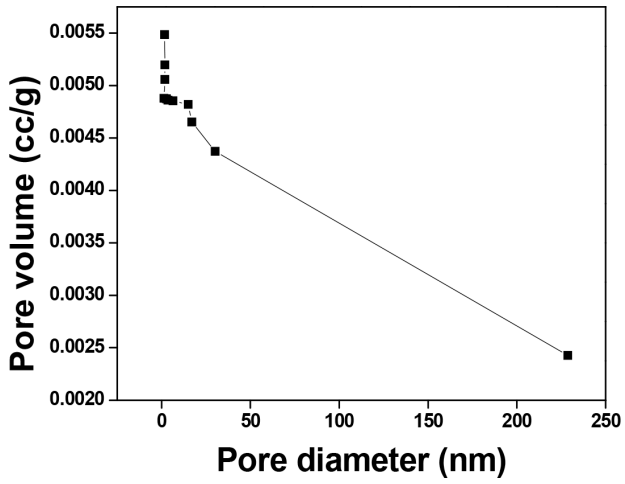

Fig. S2. Plot of pore diameter Vs pore volume.

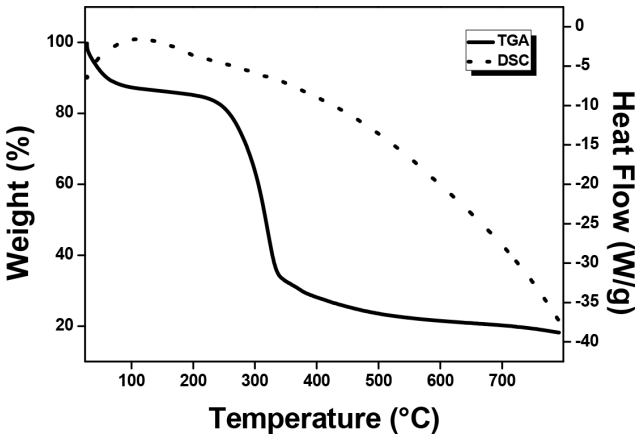

Fig. S4. TGA-DSC spectrum of raw banana fiber.

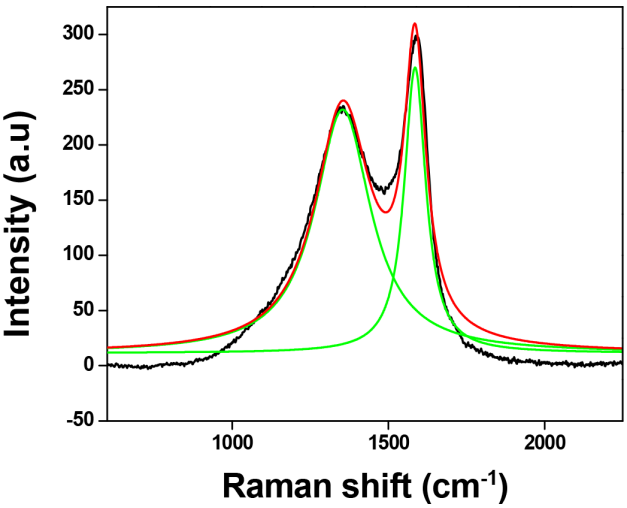

Fig. S3. Deconvoluted Raman spectrum of BFC.

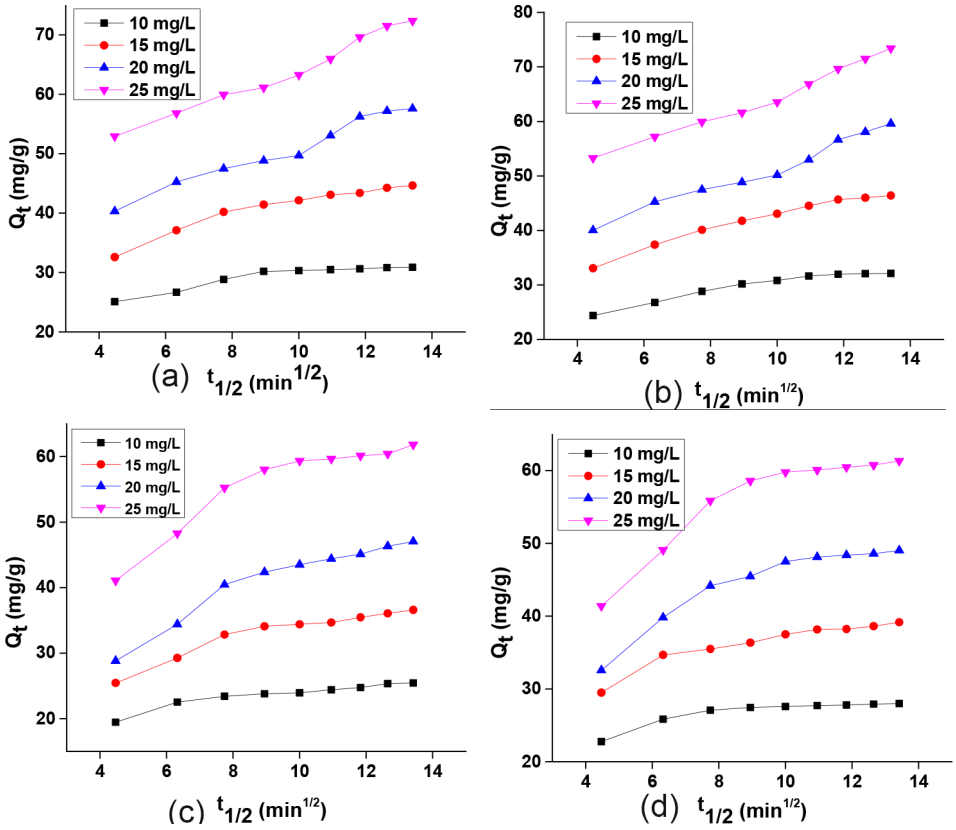

Fig. S5. Intra-particle diffusion graphs for adsorption of (A) MV, (B) MO, (C) CV and (D) ARS.